JOURNAL OF VIROLOGY, Dec. 1996, p. 8961–8971 Vol. 70, No. 12
0022-538X/96/$04.00+0

Multiple Regulatory Effects of Varicella-Zoster Virus (VZV) gL on Trafficking Patterns and Fusogenic Properties of VZV gH

KAREN M. DUUS AND CHARLES GROSE*

Department of Microbiology, University of Iowa College of Medicine, Iowa City, Iowa

Received 8 May 1996/Accepted 14 August 1996

Varicella-zoster virus (VZV) is an extremely cell-associated alphaherpesvirus; VZV infection is spread almost exclusively via cell membrane fusion. The envelope glycoprotein H (gH) is highly conserved among the herpesviruses. A virus-encoded chaperone, glycoprotein L (gL), associates with gH, and the gH:gL complex is required for gH maturation and membrane expression. We recently demonstrated that in the VZV system, the gH:gL complex facilitated cell membrane fusion and extensive polykaryon formation in transfected cells (K. M. Duus, C. Hatfield, and C. Grose, Virology 210:429–440, 1995). To further define the functions of the unusual VZV gL chaperone protein, we have performed a series of mutagenesis experiments with both gH and gL and analyzed the mutants by laser scanning confocal microscopy in a transfection-based fusion assay. We established the fact that immature gH exited the endoplasmic reticulum (ER) when coexpressed with either gE or gI and appeared on the cell surface in a patch pattern. A similar effect was observed on the cell surface with gH with a cytoplasmic tail mutagenized to closely resemble the vaccinia virus hemagglutinin cytoplasmic tail. Site-directed mutagenesis of the five gL cysteine residues demonstrated that four of five cysteines participated in the gL chaperone function required for proper maturation of gH. On the other hand, the same gL mutants facilitated transport of immature gH to the cell surface, where patching occurred. Studies of gL processing demonstrated that maturation did not require transport beyond the medial-Golgi; furthermore, gL was not detected in the outer cell membrane, nor was it secreted into the medium. Colocalization studies with 3,3′-dihexyloxa-cabocyanine iodide and *N*-(e-7-nitrobenz-2-oxa-1,3-diazol-4-yl-aminocaproyl)-D-*erythro*-sphingosine confirmed that gL was found primarily in the ER and cis/medial-Golgi when expressed alone. When all of these data were considered, they suggested a posttranslational gH:gL regulation model whereby the gL chaperone modulated gH expression via retrograde flow from the Golgi to the ER. In this schema, mature gL returns to the ER, where it escorts immature gH from the ER to the Golgi; thereafter, mature gH is transported from the trans-Golgi to the outer cell membrane, where it acts as a major fusogen.

Varicella-zoster virus (VZV), the causative agent of varicella (chicken pox) and zoster (shingles) in humans, is an extremely cell-associated member of the family *Herpesviridae*; it has no natural cell-free state in cell culture (11, 54). VZV infection in cell culture is spread as infected cells fuse with neighboring uninfected cells, forming large syncytia which eventually encompass the entire monolayer (13, 42). The genomic DNAs of the eight human herpesviruses, including that of the recently discovered Kaposi sarcoma herpesvirus (34), contain a gene encoding a highly conserved glycoprotein, gH, which is expressed on the envelopes of infectious virions and on the cell membranes of herpesvirus-infected cells (2, 3, 15, 29). The gH gene sequence is also well conserved among nonhuman herpesviruses (1, 21, 39, 41). Studies demonstrating that a single monoclonal antibody (MAb) against gH could inhibit the entry, cell-to-cell spread of infection, and egress of VZV in cultured cells have provided indirect evidence that a cell membrane fusion mechanism involving gH plays a crucial role in the VZV life cycle (7, 32, 42). Although analyses of gH deletion mutants have provided additional indirect evidence that gH plays a role in cell membrane fusion in other herpesviruses as well, additional glycoproteins appear to be required in those fusion events (50).

Efforts to express cloned gH gene products of several different herpesviruses in mammalian cells were not completely successful until Hutchinson et al. (17) identified an accessory glycoprotein gene, that for gL, of herpes simplex virus type 1 (HSV-1), the coexpression of which facilitated the processing and transport of gH to the cell surface. Unlike those of the gH genes, the gL gene sequences are not well conserved among herpesviruses. Even though the gH chaperone function of gL is maintained, the biochemistry of the gH:gL interaction appears to differ between viruses (6, 7, 17, 20, 27, 43, 49, 59). We have demonstrated the direct involvement of VZV gH in cell membrane fusion and developed a cell fusion assay; coexpression of VZV gH and gL led to extensive polykaryocytosis in transfected-cell monolayers (6). However, the question whether the gL protein itself is directly involved in the membrane fusion process is unresolved. Roop et al. (43) suggested that N-terminal amino acid residues of HSV-1 gL were responsible for complex formation with gH. Mutagenesis of cysteine residues in the C terminus of VZV gL supported this hypothesis; these mutations abolished gL-mediated gH processing, although the mutant gL molecules still associated with pre-gH (6). Other data from our earlier paper (6) supported the concept that domains required for gH:gL complex formation were distinct from those involved in the chaperone function of gL.

Because virus-mediated membrane fusion is very important in VZV infection, we investigated whether VZV gL plays an active or supportive role in VZV-mediated cell membrane fusion. Furthermore, we determined whether the domain of gL responsible for complex formation with gH was the same as that required for the chaperone function. To this end, we studied the intracellular transport of wild-type and mutated gH and gL molecules when coexpressed and individually expressed

* Corresponding author. Mailing address: University Hospital/2501 JCP, 200 Hawkins Dr., Iowa City, IA 52242-1083. Fax: (319) 356-4855. Electronic mail address: grose@blue.weeg.uiowa.edu.

TABLE 1. Antibody reagents

Antibody	Specificity
MAb 206	Mature VZV gH
MAb 3A2	VZV pre-gH and mature gH
MAb 258	Similar to that of MAb 3A2
R-60 serum	VZV gL
MAb 3B3	VZV gE; epitope-tagged gL-3B3
MAb 6B5	VZV gI

in transfected cells. Finally, we propose a model of intracellular VZV gH and gL trafficking which suggests that gL may regulate gH expression posttranslationally via retrograde flow between the Golgi apparatus and the endoplasmic reticulum (ER).

MATERIALS AND METHODS

Cells, viruses, and plasmids. HeLa cells (ATCC CCL2) were obtained from the American Type Culture Collection, Rockville, Md., and grown in Eagle minimal essential medium with 10% fetal bovine serum as previously described (57). Recombinant vaccinia virus (T7 vaccinia virus) was obtained from the laboratory of Bernard Moss at the National Institutes of Health. The eukaryotic expression vector pTM1 and the plasmids pTM1-37, pTM1-68, and pTM1-60, containing the coding sequences of the VZV gH, gE, and gL genes, respectively, were constructed as previously described (6, 7, 35, 57). The construction of pTM1-60.11 has been presented elsewhere (14). The vector pBlue-37 (also called pBlue-gpIII) contained VZV open reading frame 37 encoding gH in the pBluescript SK(+/−) plasmid (7).

Antibodies. Murine MAb 206 recognized a complement-independent neutralization epitope present on the mature gH molecule (32). MAb 3A2, which recognized an epitope present on both pre-gH and mature gH (7), was obtained from the laboratory of B. Forghani at the California Department of Health Services. Similar to MAb 3A2, MAb 258 bound to an epitope present on both mature gH and its glycosylated precursor form, pre-gH, but did not recognize unglycosylated gH precursors. The production of R-60, a rabbit polyclonal antiserum against a gL–β-galactosidase fusion protein, was described in detail by Duus et al. (6). MAb 3B3 recognized a linear epitope (amino acids 151 to 161) of VZV gE (formerly called gpI or gp98) (12, 14). MAb 6B5 bound to the ectodomain of VZV gI (formerly called gpIV or gp64) (33, 57). The properties of the antibody reagents are summarized in Table 1.

Transfection and immunoprecipitation protocols. Prior to transfection, 6×10^5 HeLa cells were seeded into six-well culture plates (Costar) and incubated overnight at 37°C in 5% CO_2. The cells were infected with T7 vaccinia virus at a multiplicity of infection of 10 and transfected with 4 μg of each plasmid as previously described (6). The transfected cells were radiolabeled overnight with 250 μCi of [^{3}H]leucine (Amersham) per ml in 2 ml of leucine-deficient medium and harvested in radioimmunoprecipitation assay buffer as previously described in detail (57). For the gL-processing study, 2 μM monensin (Sigma) was added to transfected monolayers at 7 h posttransfection and incubated overnight. To prepare the culture medium for immunoprecipitation, 2 ml of medium was removed from radiolabeled transfected HeLa cell monolayers prior to washing and harvesting of the cells. Any detached or damaged cells remaining in the medium were removed by low-speed centrifugation ($200 \times g$) for 10 min at 4°C. The medium was then concentrated 10-fold in Centricon-10 concentrator tubes (Amicon, Inc.) by centrifugation at $5,500 \times g$ at 4°C for 1 h. Cell lysates and concentrated medium were immunoprecipitated by previously described methods (32). Immunoprecipitated proteins were analyzed by gradient sodium dodecyl sulfate-polyacrylamide gel electrophoresis (SDS-PAGE) (10 to 18% polyacrylamide) under reducing (10% β-mercaptoethanol) or nonreducing conditions. Just prior to SDS-PAGE analysis, a 5-μl aliquot was removed from each sample and analyzed in a Beckman LS1801 scintillation counter to determine the counts per minute of radiolabeled protein.

For pulse-chase analyses, HeLa cell monolayers were cotransfected with gH and gL plasmids. At 4 h posttransfection the monolayers were starved for 1 h in leucine-deficient medium and pulsed with 400 μCi of [^{3}H]leucine per ml for 15 min at 37°C. The label was removed, and the monolayers were washed once with complete medium and chased in complete medium for various time periods prior to washing and harvesting in radioimmunoprecipitation assay buffer. The lysates were immunoprecipitated with an anti-gH:gL antibody cocktail containing R-60 antiserum, MAb 258, and MAb 206.

Recombination PCR site-directed mutagenesis. Site-directed mutagenesis of the VZV gH and gL genes was performed by a recombination PCR method (18, 58). Briefly, each mutagenesis reaction employed two sets of primers: nonmutating primers, described by Yao et al. (58), which bound to overlapping sequences in the ampicillin resistance genes of the vectors, and mutating primers, which bound to overlapping sequences in the gH or gL gene (Table 2). All primers were prepared by the DNA Core Facility at the University of Iowa. With one primer from each of the primer sets described above, two PCR products were generated by amplification of linearized plasmid DNA carrying the cloned gene. These products contained homologous ends; they were pooled and transformed directly into Max-Competent *Escherichia coli* DH5α (GIBCO BRL, Life Technologies). Potential clones were screened by PCR amplification and restriction enzyme digestion. Plasmid DNA from one clone carrying each mutation was isolated (INSTA-PREP; 5′-3′ Inc.), and the sequence was verified by analysis in the region of the induced mutation. DNA sequencing was performed by the DNA Core Facility at the University of Iowa. All subsequent experiments were performed with sequenced clones. As the efficiency of the in vivo recombination reaction decreased with increasing product size, the VZV gH gene was mutagenized in the pBlue-37 construct and then subcloned into the pTM1 expression vector after sequencing confirmed the presence of the mutation. Large-scale plasmid DNA isolation was performed with the Qiagen Plasmid Maxi Kit or the Qiagen EndoFree Plasmid Maxi Kit (Qiagen Inc.).

Laser scanning confocal microscopy. Transfected HeLa cell monolayers were analyzed by laser scanning confocal microscopy as previously described (6), with the following modifications. Approximately 6×10^5 HeLa cells per well were seeded into six-well culture plates. One day later, the monolayers were infected with T7 vaccinia virus at a multiplicity of infection of 10 and transfected with 15% Lipofectin and 4 μg of each DNA construct as previously described (6). To prepare transfected cells for confocal analysis, the transfected cells were fixed with 2% paraformaldehyde in 0.2 M Na_2HPO_4 for 1 h and then washed five times with phosphate-buffered saline (pH 7.4) (PBS). If the cells were to be permeabilized, 0.05% Triton X-100 was included in the fixative. The monolayers were blocked with 5% normal goat serum for 2 h at 4°C. Primary antibodies were diluted in PBS containing 1% normal goat serum: MAb 258 was diluted 1:1,600, and MAb 3B3 was diluted 1:2,500. Secondary antibodies were diluted in PBS: fluorescein-conjugated goat anti-mouse antibody (Biosource International/Tago Immunologicals) was diluted 1:1,000, and Texas red-conjugated goat anti-mouse antibody (Molecular Probes, Inc.) was diluted 1:800.

For the intracellular localization of gL-3B3, transfected HeLa cells were incubated with 0.7 mg of 3,3′-dihexyloxa-cabocyanine iodide (DiOC) (Molecular Probes, Inc.) per ml in 95% ethanol for 10 min at 37°C in the dark. The DiOC-labeled cells were fixed with 2% paraformaldehyde for 30 min, permeabilized with 0.05% Triton in 2% paraformaldehyde for 30 min, and then washed with PBS and incubated with 5% normal goat serum, as described above. After overnight incubation with primary antibody, the cells were labeled with Texas

TABLE 2. Site-directed mutagenesis of VZV glycoproteins gH and gL[a]

Primers	Amino acid change(s) (wild type→mutant)	Mutant name
5′-GGAAATAAGCGCTCTCGAAATATAATAAAAT-3′ 3′-TACAATACACCTTTATTCCGCAGAGCTTTTA-5′	S-830→K-830, L-832→S-832, E-834→K-834	gH-bt
5′-TTTTTTGCAGCTAAGCCCCTATCGGATGTG-3′ 3′-AAAAAACGTCGATTCGGGGATAGCCTACAC-5′	G-33→A-33	gL-G33A
5′-TCACAATCGCGTATGGCCTTCATCTCC-3′ 3′-AGTGTTAGCGCATACCGGAAGTAGAGG-5′	C-21→G-21	gL-C21G
5′-GATTATAACGGAGCCAGGTGTGTCATCGG-3′ 3′-TAATATTGCCTCGGTCCACACAGTAGCCAT-5′	C-48→G-48	gL-C48G

[a] The underlined nucleotides in the primer sequences encode the indicated amino acid substitutions.

Red-conjugated goat anti-mouse secondary antibody. When analyzed by laser scanning confocal microscopy, each field of interest was viewed with two filters, one to detect the DiOC, which fluoresces at the same wavelength as fluorescein, and another to detect the Texas Red label of the expressed viral glycoprotein. Photographs taken with each filter were saved on an optical disk (Panasonic), and these were electronically merged by use of the COMOS software (Bio-Rad) so that both labels were viewed simultaneously. The DiOC fluorescence was represented by a green color, and the Texas Red label of the expressed protein was represented by a red color; where the two labels colocalized, a yellow color was produced.

NBD-ceramide [*N*-(e-7-nitrobenz-2-oxa-1,3-diazol-4-yl-aminocaproyl)-D-*erythro*-sphingosine] (Molecular Probes) is a fluorescent ceramide derivative which fluoresces at the same wavelength as fluorescein (38). NBD-ceramide had been primarily employed as a vital stain to study Golgi function in living cells, but it has been shown that fixed cells could also be labeled with the dye, which preferentially stained the membranes of both the ER and Golgi (38). When cells were labeled with NBD-ceramide, bicarbonate-free Hanks' balanced salt solution (HBSS) containing 0.68 mg of fatty acid-free bovine serum albumin (BSA) (Sigma) per ml was filter sterilized and stored at 4°C. Immediately prior to labeling, 8 nmol of NBD-ceramide dissolved in 95% ethanol was added. The labeling medium was sonicated for 30 s on ice, and the tube was wrapped in aluminum foil to protect it from light. Transfected HeLa cells were incubated for 20 min at 4°C in the dark in 1.5 ml of the Hanks balanced salt solution–BSA–NBD-ceramide labeling medium. After the medium containing the NBD-ceramide was removed, the monolayers were rinsed three times with ice-cold Hanks balanced salt solution (without BSA) and chased with prewarmed Eagle minimal essential medium supplemented with 5% fetal bovine serum for 50 min at 37°C in the dark. The monolayers were examined by laser scanning confocal microscopy as described above for DiOC analysis.

RESULTS

Associations between VZV gH and VZV gE or gI. It has been well documented that the gH envelope protein of herpesviruses requires the coexpression of an accessory glycoprotein, gL, in order to be correctly processed and transported to the cell membrane (6, 7, 17, 43). In a recent report we demonstrated that a glycosylated immature form of VZV gH (pre-gH) was able to reach the cell surface in the absence of gL when coexpressed with either VZV glycoprotein gE or gI, whereupon it formed patch-like aggregations at a localized area of the cell membrane (6). The latter result suggested that the function of gL could be separated into two distinct entities: gH processing and gH transport. Immunoprecipitation of gH/gE- or gH/gI-cotransfected lysates with MAbs against gH did not demonstrate any association between pre-gH and either gE or gI (Fig. 1). As shown in Fig. 1A and B, respectively, pre-gH was coprecipitated from gH/gE- or gH/gI-cotransfected lysates with MAb 3B3 against gE or MAb 6B5 against gI. Control precipitates were included in lanes 1 and 2 of both panels of Fig. 1. Although mature gE (98 kDa) and pre-gH (97 kDa) migrated to similar positions in a 10 to 18% gradient gel (Fig. 1A, lane 3), the coprecipitation of pre-gH with gE was confirmed by immunoprecipitation of a second aliquot of gH/gE-cotransfected lysate with both MAb 3B3 and MAb 3A2 simultaneously (lane 4). No difference was seen when the double precipitation (Fig. 1A, lane 4) was compared with the single precipitation with MAb 3B3 alone (lane 3), a result which demonstrated that both glycoproteins were precipitated from the cotransfected lysate by MAb 3B3.

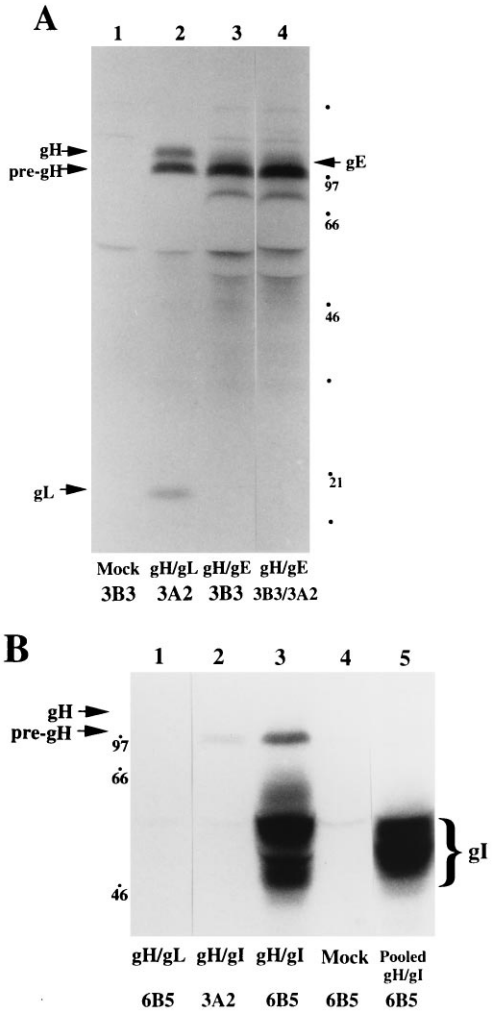

FIG. 1. Association of VZV gE and gI with pre-gH. Glycoproteins gH, pre-gH, gE, and gI are designated with arrows, and the migration of molecular mass markers (in kilodaltons) is shown in the margins. All samples were electrophoresed in the same gel. (A) Immunoprecipitation of gH/gE-cotransfected lysates. Lane 1, vaccinia virus-infected negative control precipitated with MAb 3B3 against gE; lane 2, gH/gL-cotransfected lysates precipitated with MAb 3A2 against gH; lane 3, gH/gE-cotransfected lysates precipitated with MAb 3B3; lane 4, gH/gE-cotransfected lysates precipitated with MAb 3B3 in addition to MAb 3A2. Note that gE migrates at a position between those of mature and immature gH. (B) Immunoprecipitation of gH/gI-cotransfected lysates. Lane 1, gH/gL-cotransfected lysates precipitated with MAb 6B5 against gI; lane 2, gH/gI-cotransfected lysates precipitated with MAb 3A2; lane 3, gH/gI-cotransfected lysates precipitated with MAb 6B5; lane 4, vaccinia virus-infected negative control precipitated with MAb 6B5; lane 5, individual gH-transfected and gI-transfected lysates pooled immediately after harvest and precipitated with MAb 6B5.

When gH/gI-cotransfected lysates were precipitated with MAb 6B5 against gI, several gH precursor species appeared to be coprecipitated with pre-gH and gI (Fig. 1B, lane 3). These bands were not present when HeLa cell lysates individually transfected with gH and gI genes were pooled immediately after cell lysis and then immunoprecipitated with 6B5 (Fig. 1B, lane 5). The lack of coprecipitated pre-gH in the pooled lysates demonstrated that the association between pre-gH and gI was occurring in the transfected cells and was not an artifact of cell lysis.

It was previously shown that the gH molecules expressed on the surfaces of gH/gE- and gH/gI-cotransfected cells were not completely processed (6). This lack of gH processing was also seen in the coprecipitations of gH with gE and gI (Fig. 1). The presence of aggregated pre-gH expressed on the membranes of gH/gE- or gH/gI-cotransfected cells (6), together with the above-described coprecipitation data, reaffirmed that an association occurred between pre-gH and either VZV gE or gI, which enabled pre-gH to exit the ER in the absence of gL. Digestion of the coprecipitated pre-gH/gI proteins with endoglycosidase H (endo H) revealed that the pre-gH was still endo H sensitive (data not shown). Because gE and gI were unable to mediate the final processing of gH in the Golgi apparatus, the data indicated that gL was still required for gH

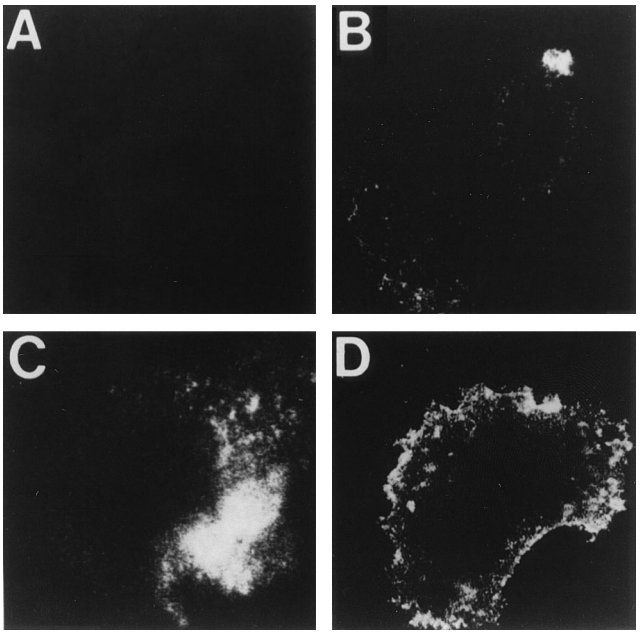

FIG. 2. Laser scanning confocal analysis of gH-bt expression. Transfected cells were incubated with primary MAb 258 against gH and a fluorescein-tagged goat anti-mouse secondary antibody. (A) Negative control. Cells transfected with the wild-type gH plasmid were permeabilized prior to staining to detect any pre-gH present in the cytoplasm. (B) Cells transfected with the gH-bt plasmid were permeabilized to detect any gH-bt in the cytoplasm. (C) Unpermeabilized gH-bt-transfected cells magnified twofold to show patching of gH-bt on the cell membrane. (D) Unpermeabilized gH-bt/gL-cotransfected cells to detect gH-bt expression on the cell surface.

maturation and suggested that gL was providing an essential gH chaperone function after pre-gH exited the ER.

Trafficking of a gH cytoplasmic tail mutation. Several reports have noted that alterations in the amino acid sequence of the cytoplasmic tail affects the intracellular trafficking and/or the cell membrane expression of viral glycoproteins (44, 47, 48, 56). These studies suggest that mutations in the gH cytoplasmic tail may generate a glycoprotein which is processed and/or transported independently of other VZV glycoproteins. The wild-type vaccinia virus hemagglutinin type 1 glycoprotein is highly charged, and it is rapidly and efficiently transported to the cell surface (47). The 14-residue VZV gH cytoplasmic tail is strikingly similar to the 13-residue tail of vaccinia virus hemagglutinin. BESTFIT analysis (Genetics Computer Group, University of Wisconsin, Madison) showed that the two sequences (VZV gH, GNSRLREYNKIPLT [3]; vaccinia virus hemagglutinin, NKRSRKYKTENKV [46]) were 43% identical. To determine if increasing the charge on the VZV gH cytoplasmic tail would render trafficking of the molecule more independent of other viral glycoproteins, a recombination PCR site-directed mutagenesis method (58) was employed to change three amino acids in the gH tail to those of the vaccinia virus tail (Table 2). The gH basic tail (gH-bt) plasmid was transfected into HeLa cells alone and cotransfected with either the VZV gL or gE plasmid. The monolayers were fixed and also permeabilized with detergent before being labeled with primary MAb 206 or MAb 258. When expressed by itself, wild-type gH was not detected in the cytoplasm of transfected cells by confocal microscopy (Fig. 2A); this result suggested that the molecule was retained and rapidly degraded in the ER, where it was not present in sufficient quantities to be detected by immunofluorescence. In contrast, when gH-bt was expressed alone, it was detected in the cytoplasm and also formed patches on the cell membrane (Fig. 2B and C) which could not be differentiated from those detected when wild-type gH was coexpressed with gE or gI (6). Confocal microscopy clearly demonstrated that increasing the charge on the cytoplasmic tail of gH enabled the molecule to exit the ER and travel to the cell membrane in the absence of other viral glycoproteins. When cotransfected with the gL gene, gH-bt cell surface expression levels and cell membrane fusion were very similar to those of wild-type gH (Fig. 2D).

However, the lack of fusion and the patching pattern of surface expression in singly transfected cells strongly suggested that the gH-bt protein was not fully processed when expressed alone. Immunoprecipitation of tritium-labeled lysates with MAb 206 and MAb 258 confirmed this suspicion; only immature pre-gH-bt was detected in cells expressing gH-bt alone, whereas both pre-gH-bt and the mature gH-bt were seen when gH-bt was expressed with gL (Fig. 3, lane 3). The pre-gH-bt mutant retained its ability to associate with gE and gI, since it was coprecipitated with either MAb 3B3 or MAb 6B5 (Fig. 3, lanes 7 and 8). As shown in Fig. 3, cotransfection of the gH-bt plasmid with either the gE or gI plasmid resulted in pre-gH-bt expression only. All pre-gH forms, including pre-gH-bt, were sensitive to digestion by endo H (reference 32 and data not shown). Thus, it was apparent that gH-bt was still dependent upon the presence of gL for processing in the Golgi. This set of experiments provided additional evidence that the critical VZV gL function with respect to gH maturation was to chaperone pre-gH in the Golgi apparatus.

Effect of gL cysteine mutations on gH maturation. The fact that the VZV gL sequence contains five cysteine residues suggests that the conformation of the molecule depends upon intramolecular disulfide bonding. Previous immunoprecipitation studies of gL molecules mutated at three C-terminal gL cysteine residues strongly suggested that the conformation of gL in the region between cysteine 79 and the C terminus was

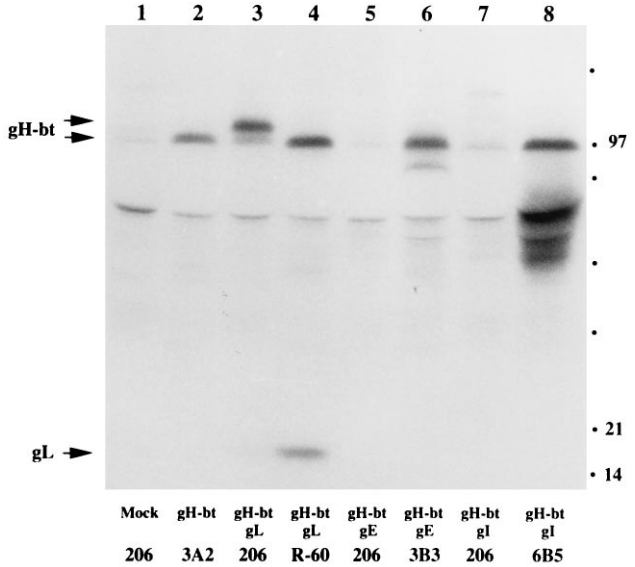

FIG. 3. Processing and complex formation of gH-bt. Transfected HeLa cell lysates labeled with [^{3}H]leucine were immunoprecipitated and analyzed by SDS-PAGE to examine the processing of gH-bt and its association with other VZV glycoproteins. The constituents of each VZV lysate preparation and the precipitating antibody are listed at the bottom of each lane. Lane 1, mock-included T7 vaccinia virus-infected HeLa cells. Numbers on the right are molecular masses in kilodaltons.

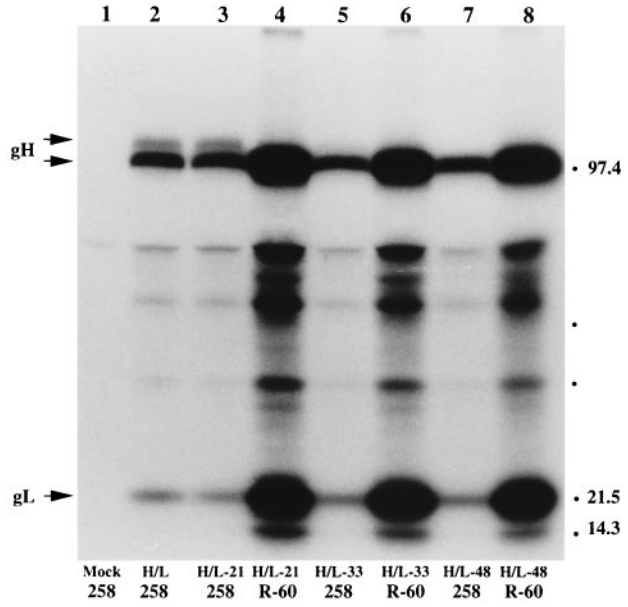

FIG. 4. Analysis of expression of gH and mutant gL proteins. Lysates of cotransfected HeLa cells labeled with [^{3}H]leucine were immunoprecipitated with MAb 258 against gH or R-60 antiserum against gL and examined for gH maturation and gH:gL complex formation. The constituents of each VZV lysate preparation and the precipitating antibody are listed at the bottom of each lane. Descriptions of mutants L-21, L-33, and L-48 are included in Results. Lane 1, mock-included T7 vaccinia virus-infected HeLa cells. Numbers on the right are molecular masses in kilodaltons.

critical for the complete processing of gH (6). Although no longer able to mediate gH maturation, these mutants retained the ability to associate with gH, as R-60 antiserum against gL still coprecipitated pre-gH with the mutant gL proteins (6). This result suggested that the N-terminal portion of gL was the pre-gH association domain. To determine if this hypothesis was correct, three additional gL mutations were generated by recombination PCR site-directed mutagenesis (58). Mutating primers were designed to construct three N-terminal gL mutations (Table 2). A glycine was substituted for cysteine 21 to generate gL-C21G, and similarly, a glycine was substituted for cysteine 48 to generate gL-C48G. Approximately midway between the two C-terminal cysteine residues, the secondary structure of gL was predicted to be helical by the DNAsis program (Hitachi Software). To generate a localized disruption of the secondary structure in the gL N terminus, an alanine residue was substituted for glycine 33 to generate the gL-G33A mutant.

These mutant gL genes were individually cotransfected into HeLa cells with the gH gene; the results are illustrated in Fig. 4. For example, gH coexpressed with gL mutant gL-C21G was indistinguishable from that expressed with wild-type gL (Fig. 4, compare lanes 2 and 3). In contrast, the amount of mature gH detected when expressed with gL-G33A was barely discernible, and only the pre-gH band was present in gH/gL-C48G-cotransfected lysates (Fig. 4, lanes 5 and 7). The absence of any mature gH expression with gL-C48G, a result indistinguishable from those seen with the gL-C79G and gL-ΔC146 mutants described by Duus et al. (6), suggested that four of the five gL cysteine residues participated in the conformation of gL required for a proper chaperone interaction with gH. On the other hand, just as with the gL-C79G and gL-ΔC146 mutants, the association between pre-gH and the three gL mutants was retained, as shown in the lanes precipitated with R-60 antiserum (Fig. 4, lanes 4, 6, and 8). The formation of complexes between pre-gH and all gL mutants indicated that this interaction was less dependent upon gL conformation and perhaps was similar to that observed between pre-gH and gE or gI.

Modulation of gH expression by mutated gL genes. To determine if the gH expressed with the three N-terminal gL mutants was transported to the surface membranes of cotransfected cells, laser scanning confocal microscopy was performed on fixed cells incubated with primary MAb 258. The transfections illustrated in Fig. 5 were performed simultaneously so that the fluorescence intensities could be directly compared. It was observed that there was either equal or increased fluorescence on the surfaces of cells cotransfected with gH and gL-C21G and a decreased surface fluorescence on gH/gL-G33A-cotransfected cells when compared with the degree of fluorescence of gH expressed with the wild-type gL (compare Fig. 5A with B and C). Thus, the confocal analysis supported the precipitation data of Fig. 4, which showed that mutation of cysteine 21 of gL was not detrimental to gH processing, whereas mutation of glycine 33 decreased gH maturation.

Interestingly, as shown in Fig. 5D, confocal analysis with MAb 258 detected the same patching phenomenon with gL-C48G that had been observed when gH was expressed with either gE or gI (6). Although previous confocal analysis of gH coexpressed with gL-C79G and gL-ΔC146 had suggested that no gH was transported to the cell membrane (6), those experiments were performed with MAb 206, which detects primarily mature gH molecules. As illustrated in Fig. 5E and F, when cell surface expression of pre-gH was probed with MAb 258, the other two maturation-deficient gL mutants, gL-C79G and gL-ΔC146, also exhibited the patching phenomenon. This result confirmed that the localized pattern of fluorescence was a specific result of pre-gH being transported to the cell membrane, as the same pattern was never detected when mature gH was expressed on the membrane. Thus, confocal analysis of gH expression with the gL mutants confirmed the immunoprecipitation data and provided further evidence that the gL sequence between residue 48 and the C terminus was important for the gL chaperone-assisted maturation of gH.

Processing and trafficking of VZV gL. Previous studies of VZV gH glycosylation demonstrated that gH was sialated; therefore, it must traverse the trans-Golgi apparatus to be completely processed (32). While gL expressed in transfected cells was resistant to endo H digestion, it was sensitive to digestion by endo F, results which demonstrated that gL entered the medial compartment of the Golgi (6). To determine if gL was being processed in the trans-Golgi, gH/gL-cotransfected cells were incubated with [^{3}H]leucine in the presence of 2 μM monensin, which inhibits trans-Golgi processing. In the presence of monensin, gH immunoprecipitated with MAb 258 was not completely processed and served as the positive control (Fig. 6, lane 4). Of note, the gL molecules expressed in the presence of monensin and immunoprecipitated with R-60 antiserum showed no change from the usual SDS-PAGE migration pattern (Fig. 6, lanes 2, 3, and 4). This result indicated that gL matured in the medial-Golgi cisternae and did not require further processing in the trans-Golgi.

Although VZV gL did not require transit through the trans-Golgi for processing, it could be transported through the trans-Golgi along with gH. In a recent publication, Dubin and Jiang (5) demonstrated that HSV-1 gL alone or gL complexed with soluble gH was immunoprecipitated from the concentrated culture medium of transfected cells. To determine if VZV gL was traveling to the cell membrane and being secreted, medium removed from [^{3}H]leucine-labeled cells transfected with the gL gene alone or with both the gH and gL genes was

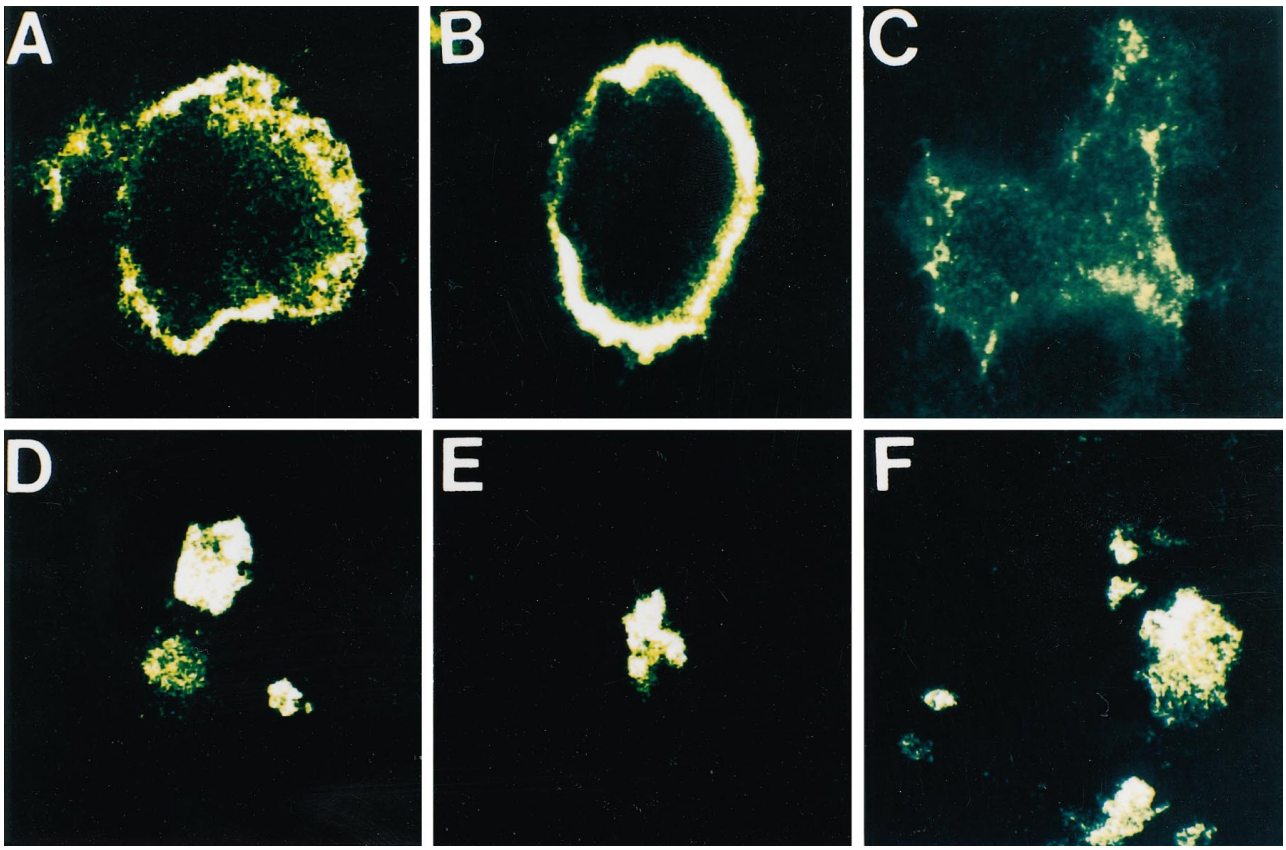

FIG. 5. Confocal microscopic analysis of gH coexpressed with five different gL mutants. Cotransfected HeLa cells were fixed (but not permeabilized) and incubated with MAb 258 in order to assess cell surface gH expression. (A) gH detected on the gH/wild-type gL-cotransfected cells; (B) gH detected on gH/gL-C21G-cotransfected cells; (C) gH detected on gH/gL-G33A-cotransfected cells; (D, E, and F) patching patterns of pre-gH expression detected on membranes of cells cotransfected with gH and gL-C48G (D), gH and gL-C79G (E), and gH and gL-ΔC146 (F). The entire experiment was performed four times; the set of micrographs shown represents one of the four experiments.

concentrated 10-fold in Centricon-10 concentrator tubes and then subjected to immunoprecipitation with either R-60 antiserum, MAb 258, or both. Cells from which the medium was concentrated were lysed and also immunoprecipitated to confirm that the proteins had been expressed. The results of this experiment are shown in Table 3 as counts per minute of detected radioisotope in 5 μl of the final 100 μl of the protein A-Sepharose eluate. The counts per minute in concentrated medium from transfected cells were not significantly different from those in the mock-transfected cell control lysates (Table 3), a result which demonstrated that VZV gL was not being secreted into the culture medium in either the presence or absence of gH. Thus, these results strongly suggested that VZV gL, unlike its HSV-1 homolog, remained in the cytoplasm of both transfected and cotransfected cells.

Confocal analysis of epitope-tagged gL expression. Investigation of the intracellular localization of gL via confocal microscopy presented a methodological problem, as the R-60 antiserum against gL had a high level of background fluorescence (data not shown). To circumvent this problem, gL was tagged with an 11-residue linear epitope of VZV gE recognized by MAb 3B3 (14). This epitope is highly resistant to denaturation (12). The epitope was inserted in frame into the gL gene, immediately C terminal to the cysteine 21 codon, by a recombination PCR mutagenesis method (14). The resulting construct, pTM1-60.11, was cotransfected into HeLa cells with the gH plasmid and analyzed by confocal microscopy with

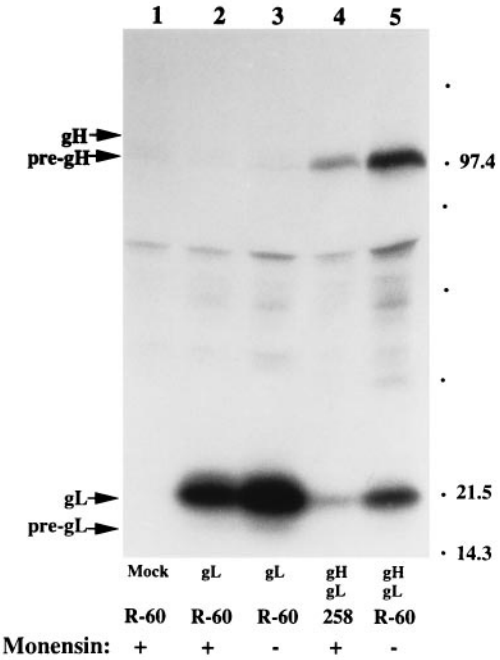

FIG. 6. Effect of monensin on gL processing. HeLa cells were transfected with gH and/or gL genes in the presence (+) or absence (−) of 2 μM monensin. The antigens and precipitating antibody used are listed at the bottom of each lane. Lane 1, mock-included T7 vaccinia virus-infected HeLa cells treated with monensin. Numbers on the right are molecular masses in kilodaltons.

TABLE 3. Amounts of VZV gL in cell lysates and culture media

Antigen source	Antibody	cpm[a]
Medium from gL-transfected cells[b]	R-60	126
Lysate of gL-transfected cells[c]	R-60	4,165
Medium from mock-transfected cells[d]	R-60	93
Lysate of mock-transfected cells	R-60	660
Medium from gH/gL-cotransfected cells	R-60	116
Lysate of gH/gL-cotransfected cells	R-60	2,392
Medium from mock-transfected cells	3B3	89
Lysate of mock-transfected cells	3B3	551
Medium from gL-3B3-transfected cells	3B3 + R-60	138
Lysate of gL-3B3-transfected cells	3B3	3,423
	R-60	3,336
Lysate of gH/gL-3B3 cotransfected cells	3B3	2,450
Medium from gH/gL-3B3 cotransfected cells	Cocktail[e]	87

[a] Precipitated [^{3}H]leucine-labeled proteins were eluted into 100 μl of loading buffer. Five microliters was removed, and the radioactivity in 2 ml of scintillation fluid was counted.

[b] Two milliliters of medium was concentrated 10-fold and immunoprecipitated.

[c] Cells were lysed in 600 μl of radioimmunoprecipitation assay buffer, and 200 μl of unconcentrated lysate was immunoprecipitated.

[d] Cells infected with T7 vaccinia virus only were a negative control.

[e] R-60 antiserum, MAb 258, and MAb 3B3.

MAb 258 against gH. The resulting large, brightly stained polykaryon shown in Fig. 7A was indistinguishable from those formed when gH was expressed with wild-type gL. Thus, this fusion assay provided evidence that the epitope tag did not impair gL function, and it confirmed previous immunoprecipitation data (14). The location of an epitope tag nearer the N terminus of gL had an additional advantage in that it provided an internal control for R-60 antiserum precipitation experiments, since the latter antibody recognized a C-terminal sequence of gL (6).

By employing MAb 3B3 to detect the epitope-tagged gL molecule gL-3B3, we demonstrated conclusively that VZV gL was not present on the surfaces of gH/gL-3B3-cotransfected cells (Fig. 7B). When cells transfected with the gL plasmid were permeabilized, intense fluorescence was detected in the cytoplasm, often in a triangular pattern (Fig. 7C). The shape and location of the fluorescence pattern suggested that gL-3B3 was sequestered mainly in the ER of the transfected cells when expressed by itself (26). Interestingly, gL trafficking was altered when gH was coexpressed with gL-3B3 (Fig. 7D). Again, intense fluorescence was detected in restricted regions of the cytoplasm in cells presumably expressing gL-3B3 alone, as demonstrated by the brightly stained single cell in Fig. 7D. Rather than having the localized pattern of gL-3B3 expressed

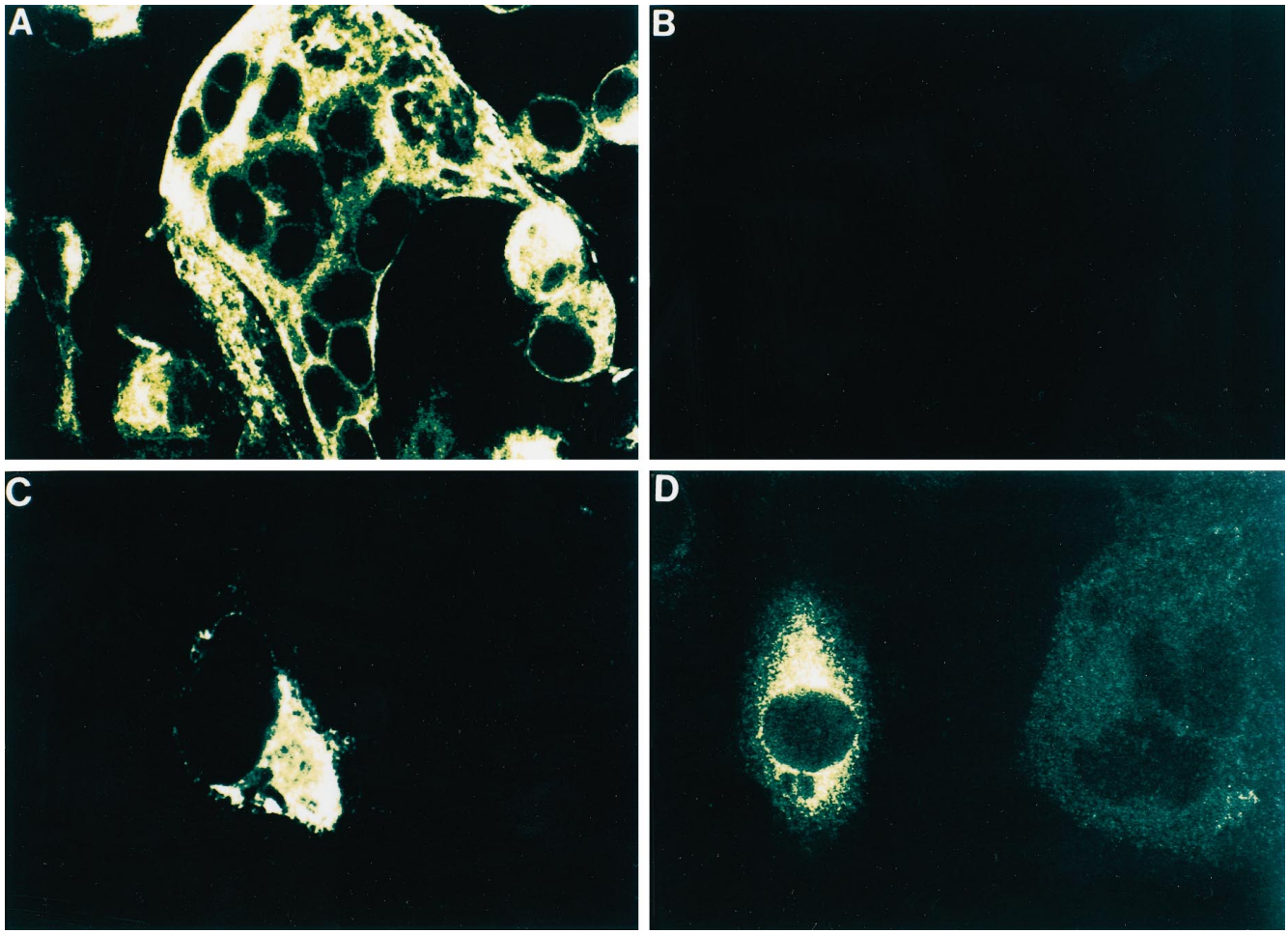

FIG. 7. Confocal microscopic analysis of epitope-tagged gL-3B3 expression. HeLa cells transfected with gH/gL-3B3 constructs or the gL-3B3 plasmid alone were incubated with primary antibody and a fluorescein isothiocyanate-tagged goat anti-mouse antibody. (A) A polykaryon formed by cotransfection with gH and gL-3B3 and detected with MAb 258; (B) absence of gL surface expression in an unpermeabilized gH/gL-3B3-cotransfected cell monolayer; (C) expression of gL-3B3 alone in permeabilized cells labeled with MAb 3B3; (D) expression of gL-3B3 together with gH after labeling with MAb 3B3.

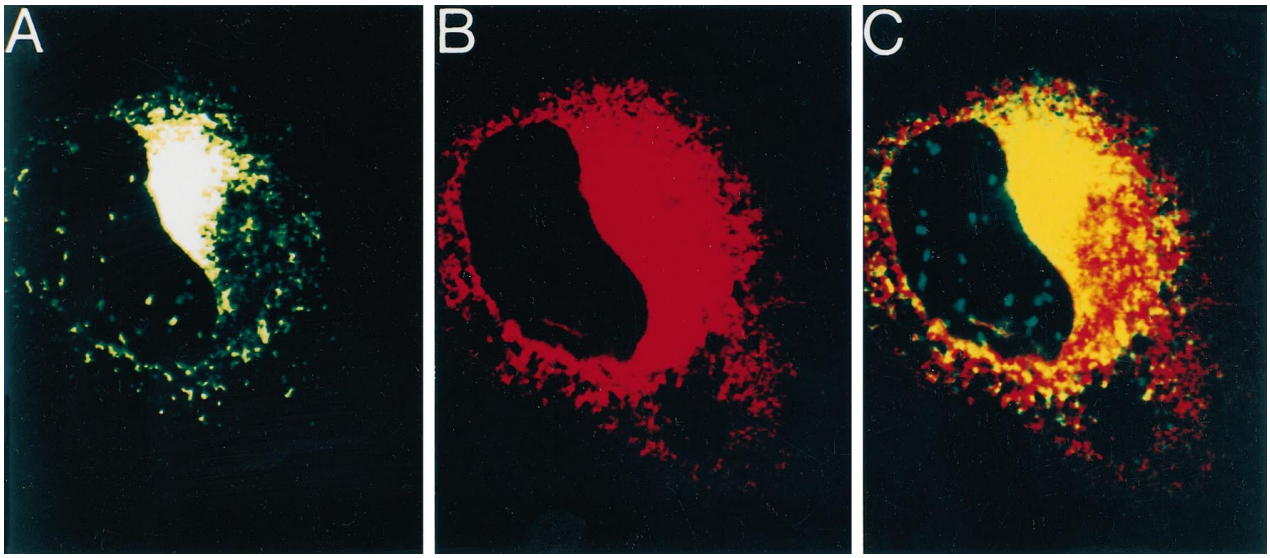

FIG. 8. Colocalization of VZV gL-3B3 with DiOC in the ER of a single transfected cell. At 18 h posttransfection, gL-3B3-transfected cells were labeled with DiOC and incubated for 10 min at 37°C immediately prior to fixation. Transfected VZV proteins were detected with a Texas Red-tagged goat anti-mouse secondary antibody. At the same time, DiOC labeling of the ER was detected by a filter measuring light emitted after laser excitation of the DiOC. (A) Fluorescence emitted by DiOC excitation, represented by a green color; (B) fluorescence emitted by Texas Red excitation, represented by a red color; (C) colocalization of the red and green signals of panels A and B, represented by a yellow color when electronically merged.

alone, the label was very diffusely distributed throughout the cytoplasm of the cotransfected cells (Fig. 7D). That these cells were cotransfected was evident by formation of a multinucleated polykaryon, which could only occur if gH and gL-3B3 were coexpressed (6). The diffuse pattern of fluorescence indicated that gL-3B3 was no longer sequestered in a particular intracellular compartment when gH was present but was distributed throughout the cytoplasm. The lower intensity of the cytoplasmic fluorescence in polykaryons also suggested that gL-3B3 was less abundant in cotransfected cells. The tagged gL-3B3, like the wild-type protein, was not detected by MAb 3B3 or R-60 in the concentrated medium of gL-3B3-transfected or gH/gL-3B3-cotransfected cells (Table 3); this result indicated that the lower intensity of the fluorescence signal in the presence of gH was not due to secretion of the gL-3B3 protein.

Colocalization of gL-3B3 and DiOC in the ER. The triangular shape, intracellular location, and intensity of the fluorescence label detected in cells expressing gL-3B3 alone was indistinguishable from the pattern of fluorescence detected by Lippincott-Schwartz et al. (26) with antiserum against ER resident proteins; this pattern suggested that gL-3B3 was localized primarily to the ER (26). In order to determine whether this hypothesis was correct, transfected cells were stained with DiOC prior to fixation and immunolabeling with MAb 3B3. DiOC, which enters intracellular organelles via proton pumps, has been shown to stain portions of the ER compartment, as well as mitochondria (53). Double or two-color staining with DiOC and a Texas Red-tagged goat anti-mouse antibody demonstrated that gL-3B3 and DiOC colocalized to the ER of gL-3B3-transfected cells (Fig. 8). The two digital images in Fig. 8A and B were merged to form one two-color image; the yellow color represented the areas of the merged image where both signals colocalized. The yellow color in the cell shown in Fig. 8C encompassed the entire region stained green by DiOC and confirmed that gL-3B3 was present in the ER of gL-3B3-transfected cells. The yellow color indicated that both signals were localized to the ER. Furthermore, the cell in Fig. 8C shows additional signal which did not colocalize to the portion of the ER compartment stained by DiOC. This staining pattern suggested that the gL was also found in the cis/medial-Golgi compartment, as would be expected if gL entered this organelle for processing. Thus, the lack of gL secretion into the medium, the absence of gL on the cell surface, and the localization of gL to the ER (in the absence of gH) provided further evidence that gL was returning to the ER after maturing in the Golgi, in order to associate with pre-gH and chaperone it through the Golgi apparatus.

Colocalization of gL-3B3 and NBD-ceramide in the ER and Golgi. As the next step, gL-3B3-transfected cells were labeled with NBD-ceramide, a fluorescent ceramide derivative which preferentially stains both ER and Golgi organelles. NBD-ceramide labeling of the ER and Golgi was detected by examining cells with a filter which detected the light emitted by the laser excitation of the NBD-ceramide. The same cells were immediately examined with a second filter which detected the light emitted by the Texas Red label conjugated to the secondary goat anti-mouse antibody bound to MAb 3B3. These two digital images were then merged to form a two-color image. The yellow color in Fig. 9A occurred over the entire region stained by NBD-ceramide. This result confirmed the DiOC data that gL-3B3 was being sequestered in the ER of gL-3B3-transfected cells and demonstrated that gL-3B3 was also entering the Golgi apparatus. When gH/gL-3B3-cotransfected cells were double labeled with NBD-ceramide and MAb 258 against gH (Fig. 9B), the signals again colocalized to the ER and Golgi, as expected, since pre-gH must traverse these organelles to reach the cell membrane. The red color in Fig. 9B represented the presence of both pre-gH and gH recognized by MAb 258; the signal was found throughout the cytoplasm in a pattern different from that formed by MAb 3B3 labeling of gL-3B3 in Fig. 9A. Thus, the localization of gL-3B3 to the ER and Golgi in the absence of gH, and its diffuse signal when coexpressed with gH, provided additional evidence that gH maturation required the return of gL to the ER.

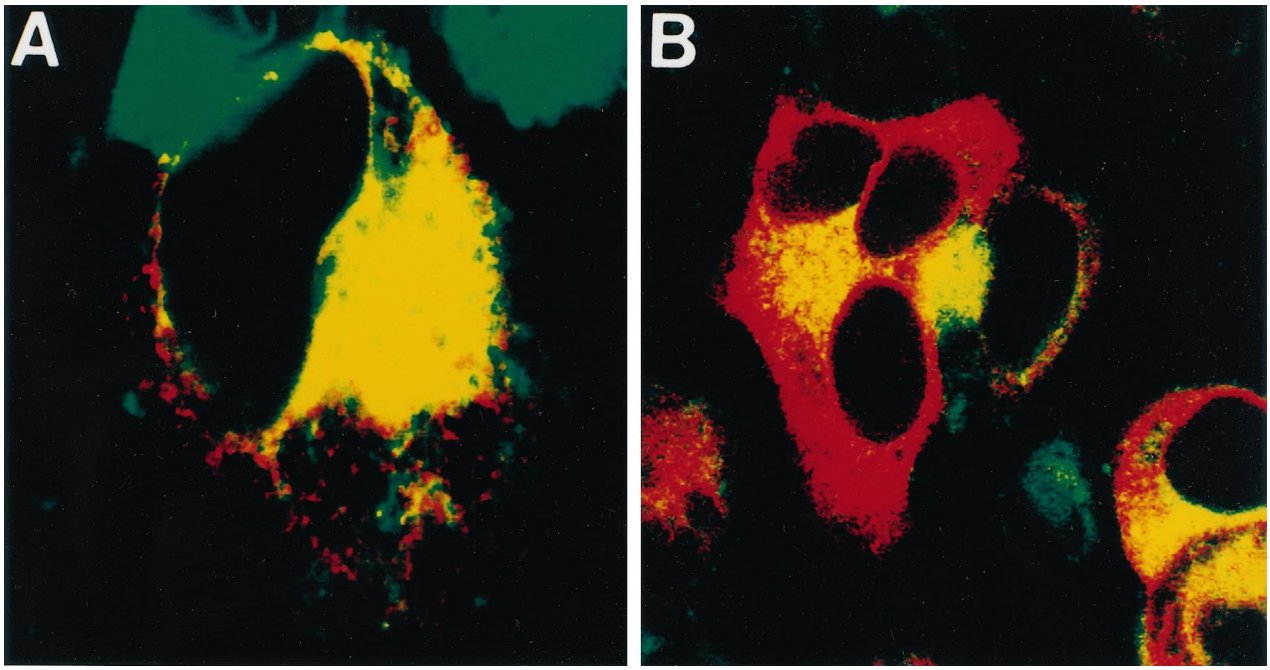

FIG. 9. Colocalization of VZV proteins with NBD-ceramide in the ER and Golgi of transfected cells. At 18 h posttransfection, cells transfected with the gL-3B3 or gH/gL-3B3 plasmid were incubated with NBD-ceramide and a MAb prior to examination by confocal microscopy. (A) Cell transfected with gL-3B3 and double labeled with MAb 3B3 (red) and NBD-ceramide (green). Colocalization of gL with NBD-ceramide is demarcated by a yellow color. (B) Polykaryon expressing gH and gL-3B3 and double labeled with MAb 258 (red) and NBD-ceramide (green). Colocalization of gH and NBD-ceramide is demarcated by a yellow color.

DISCUSSION

Many studies have characterized the cell-associated nature of VZV and its dependence on the fusion of contiguous cells for the spread of infection (13, 18, 42, 59). VZV has the smallest genome of the eight human herpesviruses, encoding fewer glycoproteins than those specified by HSV-1 (3). Furthermore, the cytopathic effects of VZV infection are more associated with syncytia or polykaryon formation than those of HSV-1. The results in an earlier study (6) and the results of this investigation provided several lines of evidence that the protein entity primarily responsible for cell membrane fusion mediated by VZV was gH. Our data proved that processing of gH to its mature glycosylated form was essential for its fusogenic function. MAb 206, which recognizes an epitope on the mature gH form, can block fusion and the cell-to-cell spread of infectivity, even when added by itself into the medium overlying an infected culture (42). The addition of the same MAb to gH:gL-transfected cells also blocked the fusogenic process (data not shown). Certainly, the gH:gL complex plays a critical role in the VZV life cycle. Many studies of fusion in other herpesviruses have concluded that more than one glycoprotein is involved in fusion events (50). Therefore, we raise the distinct possibility that the fusogenic properties of VZV gH are not entirely conserved in HSV-1 gH.

Although the molecular mechanism of herpesvirus-mediated membrane fusion is not understood (50), it is not dependent upon an acidic pH as is the fusion mediated by the spike protein fusogens of rhabdovirus, orthomyxovirus, and togavirus (10, 24). VZV gH-mediated fusion may be more similar to that of paramyxovirus and retrovirus, which occurs at neutral pH and is believed to act directly on the cell membrane (37, 55). Unregulated intracellular expression of a mature fusogenic protein would be disadvantageous to the virus because the gH proteins harbor potent virus-neutralizing epitopes (9, 31, 32, 36). Indeed, Li et al. (23) recently demonstrated that human cytomegalovirus resistance to gH neutralization antibodies correlated with reduced gH expression in the envelope, and they suggested that the level of gH expression in the human cytomegalovirus viral envelope was regulated by environmental conditions. Neither studies of the HSV-1 gH promoter (51) nor studies of gH mRNA stability (16) have provided any evidence of exceptional transcriptional regulation of the gH gene. The lack of transcriptional regulation implies that gH is regulated posttranslationally. Therefore, coexpression of gL may be a posttranslational mechanism by which gH expression is regulated.

VZV gL was demonstrated to differ from HSV-1 gL in at least three characteristics: (i) VZV gL did not associate with the mature gH molecule; (ii) it was not secreted into the medium of transfected cells when expressed by itself but was sequestered in the ER; and (iii) although gL processing occurred independently of gH expression, its sequence contained neither a typical N-terminal ER signal sequence nor a consensus signal peptide cleavage site (6). Since VZV gL is about one-half the size of HSV-1 gL, the former may have retained the chaperone properties of its larger homolog while shedding other, as-yet-undetermined properties of HSV gL. VZV gL does contain a 16-residue sequence (residues 72 to 87) common to members of the ER-targeting family of proteins (4, 6, 8). This sequence is thought to enable nascent ER resident proteins without signal peptides to be targeted to the ER. While performing homology searches on the Marek's disease virus homolog of gL, Yoshida et al. (60) observed a stretch of 28 amino acids (VZV gL residues 73 to 100) which were highly conserved between Marek's disease virus, VZV, HSV-1, and equine herpesvirus type 1. All but the first residue of the 16-amino-acid ER-targeting sequence of VZV gL are included in this conserved region.

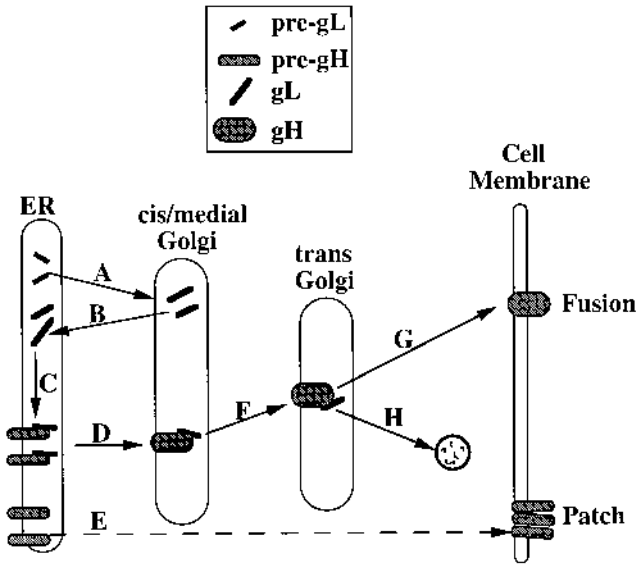

FIG. 10. Model of posttranslational regulation of VZV gH expression by VZV gL. The model proposes basically three trafficking patterns: (i) trafficking of mature gH from the ER to the cell surface (fusion) with a functional gL chaperone, (ii) possible retrograde transport of gL to chaperone gH, and (iii) an alternative pathway by which immature gH can reach the cell surface (patch) without its authentic gL chaperone. A, Transport of pre-gL to the cis/medial-Golgi; B, transport of mature gL from the Golgi to the ER; C, formation of the mature gL:pre-gH complex in the ER; D, transport of mature gL:pre-gH to the cis/medial-Golgi; E, transport of pre-gH to the outer cell membrane, where patching occurs; F, maturation of gH in the trans-Golgi and trans-Golgi network; G, transport of mature gH to the cell surface, where cell-to-cell fusion occurs; H, possible degradation of mature gL within the cytoplasm.

A proposed model of posttranslational regulation of VZV gH expression by VZV gL is illustrated in Fig. 10. In particular, the model must account for the detection of a pre-gH:mature gL complex as opposed to pre-gH:pre-gL or mature gH:mature gL complexes in cotransfected cells. As illustrated in Fig. 10, we speculate that nascent gH and gL precursors enter the ER, where pre-gH is retained. Meanwhile, pre-gL exits the ER and traverses the cis/medial-Golgi compartments, where it matures. We suggest that mature gL then recycles to the ER via retrograde transport, on the basis of the immunoprecipitation and confocal colocalization studies described above. This temporal sequence also fits with pulse-chase analyses (reference 32 and unpublished data) which showed that gL matured within 30 min whereas gH required 2 h. The mature gL molecules returning to the ER associate with the retained gH precursor, and this heterodimer exits the ER and traverses the Golgi, allowing gH to mature. The mature gH molecule then dissociates from gL and continues to the cell membrane, where it becomes a fusogen. At this stage gL may be degraded, since the gL-specific fluorescence signal in the cotransfected cells was markedly reduced. Figure 10 also includes an as-yet poorly defined pathway by which immature gH exits the ER and travels without further processing to the cell surface, where it forms patches. The elucidation of many potential steps in Fig. 10 has been aided to a considerable degree by laser scanning confocal microscopy; for example, discrimination between the fusion phenomenon and the previously unrecognized patching phenomenon would never have been uncovered with conventional fluorescence scanning.

An important remaining question concerns the mechanism by which recycling of gL back to the ER is mediated (25, 26). Unlike gL, ER-resident proteins usually contain one of two well-characterized retention-retrieval signals at the C terminus, which allow receptors within the retrograde transport vesicles of the Golgi apparatus to return them to the ER should they escape (22, 25, 30, 40). An exception to this rule is a rotavirus capsid glycoprotein retained in the ER prior to capsid assembly; it contains an ER retention signal within the first 31 residues of the N terminus (28). A similar ER retrieval signal would provide an explanation for the unusual N terminus of gL and its lack of an N-terminal ER signal peptide cleavage site. The interesting suppressive effect of the gL-G33A mutation could be partially explained by the existence of an ER retrieval sequence within the N terminus of gL; a glycine residue of the rotavirus glycoprotein is one of three amino acids involved in ER retention (28). Another possibility is that the Golgi-to-ER retrieval signal resides within the previously mentioned sequence common to all members of the ER-targeting family of proteins, including the alphaherpesvirus gL molecules.

ACKNOWLEDGMENTS

This research was supported by USPHS grant AI22795 and a research grant from the Children's Miracle Network Telethon.

We thank the Thesis Defense Committee (K.M.D.) for review of the manuscript.

REFERENCES

1. **Baranowski, E., J. Dubuisson, S. van Drunen Littel-van den Hurk, A. Lorne Babiuk, A. Michel, P.-P. Pastoret, and E. Thiry.** 1995. Synthesis and processing of bovine herpesvirus-1 glycoprotein H. Virology **206:**651–654.
2. **Cranage, M. P., G. L. Smith, S. E. Bell, H. Hart, C. Brown, A. T. Bankier, P. Tomlinson, B. G. Barrell, and A. C. Minson.** 1988. Identification and expression of a human cytomegalovirus glycoprotein with homology to the Epstein-Barr virus BXLF2 product, varicella-zoster virus gpIII, and herpes simplex virus type 1 glycoprotein H. J. Virol. **62:**1416–1422.
3. **Davison, A. J., and J. E. Scott.** 1986. The complete DNA sequence of varicella-zoster virus. J. Gen. Virol. **67:**1759–1816.
4. **De Brabander, M. J., R. M. L. Van de Veire, F. E. M. Aerts, M. Borgers, and P. A. J. Janssen.** 1976. The effects of methyl [5-(2-thienylcarbonyl)-1*H*-benzimidazol-2-yl] carbamate, (R 17934; NSC 238159), a new synthetic antitumoral drug interfering with microtubules, on mammalian cells cultured *in vitro*. Cancer Res. **36:**905–916.
5. **Dubin, G., and H. Jiang.** 1995. Expression of herpes simplex virus type 1 glycoprotein L (gL) in transfected mammalian cells: evidence that gL is not independently anchored to cell membranes. J. Virol. **69:**4564–4568.
6. **Duus, K. M., C. Hatfield, and C. Grose.** 1995. Cell surface expression and fusion by the varicella-zoster virus gH:gL glycoprotein complex: analysis by laser scanning confocal microscopy. Virology **210:**429–440.
7. **Forghani, B., L. Ni, and C. Grose.** 1994. Neutralization epitope of the varicella-zoster virus gH:gL glycoprotein complex. Virology **199:**458–462.
8. **Fra, A., and R. Sitia.** 1993. The endoplasmic reticulum as a site of protein degradation. Subcell. Biochem. **21:**143–168.
9. **Fuller, A. O., and W.-C. Lee.** 1992. Herpes simplex virus type 1 entry through a cascade of virus-cell interactions requires different roles of gD and gH in penetration. J. Virol. **66:**5002–5012.
10. **Gaudin, Y., C. Tuffereau, P. Durrer, A. Flamand, and R. W. H. Ruigrok.** 1995. Biological function of the low-pH, fusion-inactive conformation of rabies virus glycoprotein (G): G is transported in a fusion-inactive state-like conformation. J. Virol. **69:**5528–5534.
11. **Gershon, A., L. Cosio, and P. A. Brunell.** 1973. Observations on the growth of varicella-zoster virus in human diploid cells. J. Gen. Virol. **18:**21–31.
12. **Grose, C.** 1990. Glycoproteins encoded by varicella-zoster virus: biosynthesis, phosphorylation and intracellular trafficking. Annu. Rev. Microbiol. **44:**59–80.
13. **Harson, R., and C. Grose.** 1995. Egress of varicella-zoster virus from the melanoma cell: a tropism for the melanocyte. J. Virol. **69:**4994–5010.
14. **Hatfield, C., K. M. Duus, D. H. Jones, and C. Grose.** Epitope mapping and tagging by recombination PCR mutagenesis. BioTechniques, in press.
15. **Heineman, T., M. Gong, J. Sample, and E. Knieff.** 1988. Identification of the Epstein-Barr virus gp85 gene. J. Virol. **62:**1101–1107.
16. **Henley, D. C., and J. P. Weir.** 1991. The relative stability of selected herpes simplex virus type 1 mRNAs. Virus Res. **20:**121–132.
17. **Hutchinson, L., H. Browne, V. Wargent, N. Davis-Poynter, S. Primorac, K. Goldsmith, A. C. Minson, and D. C. Johnson.** 1992. A novel herpes simplex virus glycoprotein, gL, forms a complex with glycoprotein H (gH) and affects normal folding and surface expression of gH. J. Virol. **66:**2240–2250.
18. **Jones, D. H.** 1994. PCR mutagenesis and recombination in vivo. PCR Methods Appl. **3:**S141–S148.

19. **Jones, F., and C. Grose.** 1988. Role of cytoplasmic vacuoles in varicella-zoster virus glycoprotein trafficking and virion envelopment. J. Virol. **62:** 2701–2711.
20. **Kaye, J. F., U. A. Gompels, and A. C. Minson.** 1992. Glycoprotein H of human cytomegalovirus (HCMV) forms a stable complex with the HCMV UL115 gene product. J. Gen. Virol. **73:**2693–2698.
21. **Klupp, B. G., and T. C. Mettenleiter.** 1991. Sequence and expression of the glycoprotein gH gene of pseudorabies virus. Virology **182:**732–741.
22. **Letourneur, F., E. C. Gaynor, S. Hennecke, C. Démollière, R. Duden, S. D. Emr, H. Riezman, and P. Cosson.** 1994. Coatomer is essential for retrieval of dilysine-tagged proteins to the endoplasmic reticulum. Cell **79:**1199–1207.
23. **Li, L., K. L. Coelingh, and W. J. Britt.** 1995. Human cytomegalovirus neutralizing antibody-resistant phenotype is associated with reduced expression of glycoprotein H. J. Virol. **69:**6047–6053.
24. **Li, Y., C. Drone, E. Sat, and H. P. Ghosh.** 1993. Mutational analysis of the vesicular stomatitis virus glycoprotein G for membrane fusion domains. J. Virol. **67:**4070–4077.
25. **Lippincott-Schwartz, J.** 1993. Membrane cycling between the ER and Golgi apparatus and its role in biosynthetic transport. Subcell. Biochem. **21:**95–119.
26. **Lippincott-Schwartz, J., J. G. Donaldson, A. Schweizer, E. G. Berger, H.-P. Hauri, L. C. Yuan, and R. D. Kausner.** 1990. Microtubule-dependent retrograde transport of proteins into the ER in the presence of brefeldin A suggests an ER recycling pathway. Cell **60:**821–836.
27. **Liu, D. X., U. A. Gompels, J. Nicholas, and C. Lelliott.** 1993. Identification and expression of the human herpesvirus 6 glycoprotein H and interaction with an accessory 40K glycoprotein. J. Gen. Virol. **74:**1847–1857.
28. **Maas, D. R., and P. H. Atkinson.** 1994. Retention by the endoplasmic reticulum of rotavirus VP7 is controlled by three adjacent amino-terminal residues. J. Virol. **68:**366–378.
29. **McGeoch, D. J., and A. J. Davison.** 1986. DNA sequence of the herpes simplex type 1 gene encoding glycoprotein H and identification of homologues in the genomes of varicella-zoster virus and Epstein-Barr virus. Nucleic Acids Res. **14:**111–114.
30. **Miesenböck, G., and J. E. Rothman.** 1995. The capacity to retrieve escaped ER proteins extends to the *trans*-most cisterna of the Golgi stack. J. Cell Biol. **129:**309–319.
31. **Miller, N., and L. M. Hutt-Fletcher.** 1988. A monoclonal antibody to glycoprotein gp85 inhibits fusion but not attachment of Epstein-Barr virus. J. Virol. **62:**2366–2372.
32. **Montalvo, E. A., and C. Grose.** 1986. Neutralization epitope of varicella zoster virus on native viral glycoprotein gp118 (VZV glycoprotein gpIII). Virology **149:**230–241.
33. **Montalvo, E. A., R. T. Parmley, and C. Grose.** 1985. Structural analysis of the varicella-zoster virus gp98-gp62 complex: posttranslational addition of N-linked and O-linked oligosaccharide moieties. J. Virol. **53:**761–770.
34. **Moore, P. S., S.-J. Gao, G. Dominguez, E. Cesarman, O. Lungu, D. M. Knowles, R. Garber, P. E. Pellett, D. J. McGeoch, and Y. Chang.** 1996. Primary characterization of a herpesvirus agent associated with Kaposi's sarcoma. J. Virol. **70:**549–558.
35. **Moss, B., O. Elroy-Stein, T. Mijukani, W. A. Alexander, and T. R. Fuerst.** 1990. New mammalian expression vectors. Nature (London) **348:**91–92.
36. **Nemecková, S., V. Ludvíková, L. Maresová, J. Krystofová, P. Hainz, and L. Kutinová.** 1996. Induction of varicella-zoster virus-neutralizing antibodies in mice by coinfection with recombinant vaccinia viruses expressing the gH or gL gene. J. Gen. Virol. **77:**211–215.
37. **Nussmaum, O., C. C. Broder, and E. A. Berger.** 1994. Fusogenic mechanisms of enveloped-virus glycoproteins analyzed by a novel recombinant vaccinia virus-based assay quantitating cell fusion-dependent reporter gene activation. J. Virol. **68:**5411–5422.
38. **Pagano, R. E., M. A. Sepanski, and O. C. Martin.** 1989. Molecular trapping of a fluorescent ceramide analogue at the Golgi apparatus of fixed cells: interaction with endogenous lipids provides a *trans*-Golgi marker for both light and electron microscopy. J. Cell Biol. **109:**2067–2079.
39. **Peeters, B., N. de Wind, R. Broer, A. Gielkens, and R. Moormann.** 1992. Glycoprotein H of pseudorabies virus is essential for entry and cell-to-cell spread of the virus. J. Virol. **66:**3888–3892.
40. **Pelham, H. R. B.** 1988. Evidence that luminal ER proteins are sorted from secreted proteins in a post-ER compartment. EMBO J. **7:**913–918.
41. **Pumphrey, C. Y., and W. L. Gray.** 1995. DNA sequence of the simian varicella virus (SVV) gH gene and analysis of the SVV and varicella zoster virus gH transcripts. Virus Res. **38:**55–70.
42. **Rodriguez, J. E., T. Moninger, and C. Grose.** 1993. Entry and egress of varicella virus blocked by same anti-gH monoclonal antibody. Virology **196:** 840–844.
43. **Roop, C., L. Hutchinson, and D. C. Johnson.** 1993. A mutant herpes simplex virus type 1 unable to express glycoprotein L cannot enter cells, and its particles lack glycoprotein H. J. Virol. **67:**2285–2297.
44. **Rose, J. K., and R. W. Doms.** 1988. Regulation of protein export from the endoplasmic reticulum. Annu. Rev. Cell Biol. **4:**257–288.
45. **Seraste, J., and E. Kuismanen.** 1984. Pre- and post-Golgi vacuoles operate in the transport of Semliki forest virus membrane glycoproteins to the cell surface. Cell **38:**535–549.
46. **Shida, H.** 1986. Variants of vaccinia virus hemagglutinin altered in intracellular transport. Mol. Cell. Biol. **6:**3734–3745.
47. **Shida, H.** 1986. Nucleotide sequence of the vaccinia virus hemagglutinin gene. Virology **150:**451–462.
48. **Skoff, A. M., and T. C. Holland.** 1993. The effect of cytoplasmic domain mutations on membrane anchoring and glycoprotein processing of herpes simplex virus type 1 glycoprotein C. Virology **196:**804–816.
49. **Spaete, R. R., K. Perot, P. I. Scott, J. A. Nelson, M. F. Stinski, and C. Pachl.** 1993. Coexpression of truncated human cytomegalovirus gH with the UL115 gene product or the truncated human fibroblast growth factor receptor results in transport of gH to the cell surface. Virology **193:**853–861.
50. **Spear, P. G.** 1993. Membrane fusion induced by herpes simplex virus, p. 201–232. *In* J. Bentz (ed.), Viral fusion mechanisms. CRC Press, Boca Raton, Fla.
51. **Steffy, K. R., and J. P. Weir.** 1991. Upstream promoter elements of the herpes simplex virus type 1 glycoprotein H gene. J. Virol. **65:**972–975.
52. **Steffy, K. R., and J. P. Weir.** 1991. Mutational analysis of two herpes simplex virus type 1 late promoters. J. Virol. **65:**6454–6460.
53. **Terasaki, M., and T. S. Reese.** 1992. Characterization of endoplasmic reticulum by colocalization of BiP and dicarboxycyanine dyes. J. Cell Sci. **101:** 315–322.
54. **Weller, T. H.** 1953. Serial propagation in vitro of agents producing inclusion bodies derived from varicella and herpes zoster. Proc. Soc. Exp. Biol. Med. **83:**340–346.
55. **White, J. M.** 1992. Membrane fusion. Science **258:**917–924.
56. **Wilson, D. W., N. Davis-Poynter, and A. C. Minson.** 1994. Mutations in the cytoplasmic tail of herpes simplex virus glycoprotein H suppress cell fusion by a syncytial strain. J. Virol. **68:**6985–6993.
57. **Yao, Z., W. Jackson, B. Forghani, and C. Grose.** 1993. Varicella-zoster virus glycoprotein gpI/gpIV receptor: expression, complex formation, and antigenicity within the vaccinia virus-T7 RNA polymerase transfection system. J. Virol. **67:**305–314.
58. **Yao, Z., D. H. Jones, and C. Grose.** 1992. Site-directed mutagenesis of herpesvirus glycoprotein phosphorylation sites by recombination polymerase chain reaction. PCR Methods Appl. **1:**205–207.
59. **Yaswen, L. R., E. B. Stephens, L. C. Davenport, and L. M. Hutt-Fletcher.** 1993. Epstein-Barr virus glycoprotein gp85 associates with the BKRF2 gene product and is incompletely processed as a recombinant protein. Virology **195:**387–396.
60. **Yoshida, S., L. F. Lee, N. Yanagida, and K. Nazerian.** 1994. Identification and characterization of a Marek's disease virus gene homologous to glycoprotein L of herpes simplex virus. Virology **204:**414–419.